

Published in final edited form as:

Cell Rep. 2012 September 27; 2(3): 674–684. doi:10.1016/j.celrep.2012.07.011.

Identification of cytoplasmic capping targets reveals a role for cap homeostasis in translation and mRNA stability

Chandrama Mukherjee^{1,2,3}, Deepak P. Patil^{1,2,3}, Brian A. Kennedy^{1,2,4}, Baskar Bakthavachalu^{1,2}, Ralf Bundschuh^{1,5}, and Daniel R. Schoenberg^{1,2,6}

¹Center for RNA Biology, The Ohio State University, Columbus, OH 43210

²Department of Molecular and Cellular Biochemistry, The Ohio State University, Columbus, OH 43210

⁵Departments of Physics and Biochemistry, The Ohio State University, Columbus, OH 43210

Summary

The notion that decapping leads irreversibly to mRNA decay changed with the identification of capped transcripts missing portions of their 5' ends and a cytoplasmic complex that can restore the cap on uncapped mRNAs. The current study used accumulation of uncapped transcripts in cells inhibited for cytoplasmic capping to identify the targets of this pathway. Inhibition of cytoplasmic capping resulted in the destabilization of some transcripts and the redistribution of others from polysomes to non-translating mRNPs, where they accumulate in an uncapped state. Only a portion of the mRNA transcriptome is affected by cytoplasmic capping, and its targets encode proteins involved in nucleotide binding, RNA and protein localization and the mitotic cell cycle. The 3'-UTRs of recapping targets are enriched for AU-rich elements and microRNA binding sites, both of which function in cap-dependent mRNA silencing. These findings identify a cyclical process of decapping and recapping we term cap homeostasis.

Keywords

cytoplasmic capping; cap homeostasis; translation; polysomes; mRNP; non-translating mRNA; mRNA stability; uncapped transcriptome

Introduction

The 5' end of all eukaryotic mRNAs is modified by the addition of an inverted methylguanosine 'cap'. The cap is added co-transcriptionally through the action of capping enzyme and cap methyltransferase, both of which are positioned at the 5' end of newly-transcribed pre-mRNA by the C-terminal domain of RNA polymerase II (Gu and Lima, 2005), and the quality of cap methylation is monitored by the Rat1/Rai1 complex and pre-mRNAs with improperly methylated caps degraded before they can be exported to the

© 2012 Elsevier Inc. All rights reserved.

⁶Address correspondence to: Daniel R. Schoenberg, Ph.D. Department of Molecular and Cellular Biochemistry, The Ohio State University, 333 Hamilton Hall, 1645 Neil Ave. Columbus, Ohio 43210-1218, schoenberg.3@osu.edu.

³These authors contributed equally to this work

⁴Current address: Ion Torrent, Inc., 7000 Shoreline Ct, Suite 201, South San Francisco, CA, 94080

Publisher's Disclaimer: This is a PDF file of an unedited manuscript that has been accepted for publication. As a service to our customers we are providing this early version of the manuscript. The manuscript will undergo copyediting, typesetting, and review of the resulting proof before it is published in its final citable form. Please note that during the production process errors may be discovered which could affect the content, and all legal disclaimers that apply to the journal pertain.

cytoplasm (Jiao et al., 2010). In the nucleus, the cap is bound by a heterodimer of CBP80-CBP20, and its interaction with other proteins coordinates many of the subsequent steps in pre-mRNA processing and mRNA surveillance (Schoenberg and Maquat, 2012). mRNAs are exported to the cytoplasm cap-end first, where the CBP80-CBP20 heterodimer is replaced by eIF4E, leading to translation initiation through the eIF4F complex.

Translation and mRNA decay are interconnected processes. A simplified view of mRNA decay starts with shortening of the poly(A) tail to a point where it can no longer function to support translation, followed by decapping and degradation of the mRNA with 5'-3' polarity by the Xrn1 exonuclease (Schoenberg and Maquat, 2012). In reality mRNA decay is much more complicated and can involve decapping while ribosomes are engaged in translation (Hu et al., 2009), bidirectional decay (Murray and Schoenberg, 2007; Mullen and Marzluff, 2008) and endonuclease cleavage (Schoenberg, 2011). Loss of the cap, either by hydrolysis by Dcp2 or Nud16, or by endonuclease cleavage within the body of the transcript is common to all of these. Until recently this was thought to be irreversible, with Xrn1 rapidly degrading decapped mRNAs.

This notion has begun to change, starting first with work done in *Arabidopsis* and more recently in human cells. In most of these studies the 5'-monophosphate on uncapped mRNAs were tagged by ligating to a primer for subsequent physical recovery and analysis on microarrays (Jiao et al., 2008) or for identification of 5' ends by deep sequencing (Gregory et al., 2008; Karginov et al., 2010; Mercer et al., 2010; Ni et al., 2010). These studies identified an uncapped transcriptome that contained a significant representation of protein-coding transcripts. In addition to finding transcripts with nearly intact 5' ends, work in mammalian cells also found widespread evidence for endonuclease cleavage that was independent of Drosha, Dicer and RISC (Karginov et al., 2010). It has yet to be determined if these uncapped transcripts represent intermediates in the decay process, intermediates in (or products of) the generation of regulatory RNAs, or new forms of mRNAs that are capable of encoding N-terminally truncated proteins. There is precedent for the latter from work using antisense oligonucleotides (Thoma et al., 2001), where stable transcripts that accumulate downstream of antisense oligonucleotide cleavage were translated into new protein products. The latter was a mystery, as the targets lacked an internal ribosome entry site and there was no precedent for restoring a cap on decapped or endonucleolytically-cleaved RNAs.

In erythroid cells the decay of nonsense-containing beta-globin mRNA is accompanied by the appearance of stable truncated transcripts that retain their poly(A) tail but are missing sequences from the 5' end (Lim et al., 1992). These are generated by endonuclease cleavage (Bremer et al., 2003; Stevens et al., 2002), and were reported to be modified with a 5' cap or cap-like structure (Lim and Maquat, 1992), a finding that we confirmed (Otsuka et al., 2009). This finding also raised the question how cap addition might occur in the cytoplasm, since capping enzyme was thought only to be in the nucleus and if there was a cytoplasmic pool one would still be faced with the problem of converting the 5'-monophosphate ends generated by endonuclease cleavage to a diphosphate capping substrate. These questions were resolved by our identification of a ~140 kDa complex containing capping enzyme complex and the requisite kinase (Otsuka et al., 2009).

Capping enzyme cannot be knocked down without cell death (Chu and Shatkin, 2008). To circumvent issues associated with altering nuclear capping we developed forms of capping enzyme that are restricted to the cytoplasm, one of which is inactive as a consequence of changing the GMP-binding site at K294 to alanine (K294A). We showed in Otsuka et al. (2009) that this form of capping enzyme is incorporated into the cytoplasmic capping enzyme complex, and its overexpression reduced the ability of cells to recover from arsenite

stress. Because recovery from stress depends on the restoration of cap-dependent translation (Anderson and Kedersha, 2002) this suggested the overexpressed K294A form of capping enzyme may have blocked the recapping of uncapped transcripts that may have accumulated under these conditions. The current study used the accumulation of uncapped transcripts in cells overexpressing K294A to identify cytoplasmic capping targets. In the process we found that cytoplasmic capping affects the stability of some mRNA and the translation of others, particularly mRNAs that encode proteins associated with the mitotic cell cycle.

Results

Identification of recapping substrates

We previously described lines of tetracycline-inducible cells expressing wild type (CE Δ NLS+NES) and inactive (K294A Δ NLS+NES, referred to from here on as K294A) forms of capping enzyme that were modified to restrict their distribution to the cytoplasm (Otsuka et al., 2009). As noted above, K294A is incorporated into the cytoplasmic capping enzyme complex and its overexpression reduced the ability of cells to recover from arsenite stress. We interpreted this as evidence for inhibition of cytoplasmic capping, and the data suggested that cell death might result from reduced reactivation of translationally-silenced mRNAs. Based on this logic, the K294A cell line was used as an isogenic system for identifying mRNA targets of cytoplasmic capping.

The targets of cytoplasmic capping were identified using Affymetrix Human Exon 1.0 ST microarrays, with the resulting hits mapped to the Ensembl GRCh37 Release 60 reference assembly. To limit this analysis to validated transcripts only those with an annotation status of “known” were considered, and any probes within a probeset that did not map completely and uniquely to the target transcript were removed from consideration, resulting in a working data set of 55,662 transcripts. Analysis of mean signal intensity of each probeset as a function of its location relative to the 5' ends of mapped transcripts showed minimal overall impact of K294A expression (Fig. S1A), with the slightly lower regression line suggesting some transcripts might be reduced in these cells.

In Otsuka et al. (2009) the *in vitro* susceptibility to a 5'-3' exonuclease proved to be an effective method of discriminating between capped and uncapped RNAs. A similar approach was used on a global scale to identify uncapped RNAs and changes in cap status (Fig. 1A). Triplicate cultures were maintained for 24 h in medium \pm doxycycline where K294A is maximally induced, and cytoplasmic RNA from each culture was depleted of ribosomal RNA prior to treating one half of each preparation with Xrn1. The RNA recovered from each treatment group was then applied to separate microarrays. As expected, the majority of the mRNA transcripts present in control and induced cells were capped and hence resistant to Xrn1, and typical results for such RNAs are in Fig. S1B.

Under these conditions most uncapped transcripts were partially degraded, and only with rare exceptions were uncapped RNAs degraded completely. An independent T-test was used to assess differences between the 5' and 3' ends, and Benjamini-Hochberg family wise error correction was used to limit hits to transcripts whose difference between treatment groups had $p < 0.05$ (see Supplementary Experimental Procedures). This identified 2666 transcripts from control cells with some degree of susceptibility to degradation by Xrn1 (Fig. 1B). We refer to these as the ‘uninduced’ set, and based on their similarity to products identified in Mercer et al. (2010) and Karginov et al. (2010) represent natively uncapped transcripts. Another 675 transcripts were identified that are unique to K294A-expressing cells. These are referred to as the ‘capping inhibited’ set. Lastly 835 transcripts were identified that had some degree of Xrn1 susceptibility in control cells, and increased Xrn1 susceptibility in

K294A-expressing cells. These are referred to as the 'common' set. A graphical representation of microarray data for one of these is in Fig. S1C.

The differential Xrn1 susceptibility of each set of transcripts is shown by heat map in Figs. 1C–E. The 2666 transcripts of the uninduced set are shown in Fig. 1C, with individual transcripts arrayed down the Y axis and differences in probe intensity for the first 1500 nucleotides arrayed across the X axis. While the decreased intensity of the 5' probe sets following Xrn1 digestion is consistent with the presence of uncapped forms of each of these mRNAs more compelling results are seen by comparing the Xrn1 susceptibility of the 835 common transcripts recovered from uninduced (–Dox) and K294A-expressing (+Dox) cells (Fig. 1D, left versus right panels). The same transcripts are aligned horizontally, and the greater Xrn1 susceptibility of transcripts recovered from K294A-expressing cells is consistent with an increase in the proportion of uncapped mRNAs. Finally, Fig. 1E shows the heat map of the 675 capping inhibited transcripts, which are susceptible to Xrn1 only when they are recovered from K294A-expressing cells. This is notable for its similarity to the heat map of the common transcripts recovered from K294A-expressing cells (Fig. 1D, right panel), suggesting that uncapped mRNAs accumulate in these cells as a consequence of K294A expression.

Xrn1 susceptible transcripts are uncapped

Eleven putative recapping targets made up of transcripts from the common and capping inhibited set (Table S1) were selected for detailed analysis of changes in cap status as a function of K294A expression, and in the following experiments these were compared to five Xrn1-resistant controls. The first experiment again used Xrn1 susceptibility as a measure of cap status (Fig. 2A), except that changes were assayed by qRT-PCR using primers located near the 5' ends of each transcript. A difference coefficient was computed by comparing the ratio of Xrn1 susceptibility between treatment groups such that a value of 1 indicates no change and a number greater than 1 indicates the relative increase in susceptibility. Expression of K294A had no impact on the Xrn1 susceptibility of any of the 5 control transcripts, but Xrn1 sensitivity increased for each of the putative recapping targets (Fig. 2A), a result that is consistent with an increase in uncapped forms of these mRNAs.

Three additional approaches were used to confirm the appearance of uncapped forms of recapping targets in K294A-expressing cells, each of which included a normalization control of uncapped human β -globin RNA that was spiked into each RNA preparation. The first used a modification of an approach designed to tag, recover and identify uncapped mRNAs from *Arabidopsis* (Jiao et al., 2008). In this an RNA adapter is ligated to the 5'-monophosphate end of uncapped RNAs, followed by hybridization to a complementary biotinylated DNA oligonucleotide, and recovery on streptavidin paramagnetic beads. Changes in recovery as a function of K294A expression were determined as above by qRT-PCR, with results normalized to the β -globin control (Fig. 2B). The increased recovery of recapping targets from RNA of K294A-expressing cells compared to RNA of control cells is consistent with the results of Xrn1 digestion and support the results of microarray experiments for accumulation of uncapped forms of the recapping targets.

The preceding approaches are indirect methods for assessing the accumulation of uncapped RNAs. To look directly for changes in uncapped RNA we performed 5'-RACE using the adapter-ligated RNA from Fig. 2B and primers for each of the recapping targets as well as the internal β -globin control (Fig. 3A). Eight of the recapping targets produced detectable RACE products, and in each case these were more pronounced with RNA from K294A-expressing cells than from control cells. Moreover, the similarity in RACE products from the uncapped β -globin control (bottom right panel) confirms that the differences observed here result from increases in the amount of each of these that is uncapped.

The final evidence that uncapped transcripts accumulate in K294A-expressing cells came from differences in binding to a cap affinity resin. We showed previously that approximately 30% of capped RNA can be recovered on immobilized eIF4E or a trimethyl cap monoclonal antibody (Otsuka et al., 2009). To improve on this we generated a cap affinity resin consisting of the heterodimer of eIF4E bound to the eIF4E-binding domain of eIF4G. This resin binds 60–90% of capped RNAs (see Supplemental Experimental Procedures) and none of the uncapped β -globin RNA control. RNA recovered in the unbound fraction was normalized to the internal β -globin standard, and differences were expressed as the value for a particular transcript in RNA from control versus K294A-expressing cells (Fig. 3B). Consistent with differences in capping, expression of K294A increased the proportion of recapping target transcripts in the unbound fraction but had little impact on recovery of each of the 5 control transcripts. Together these 4 independent assays of cap status support the conclusion that cytoplasmic capping is inhibited by K294A expression, and uncapped transcripts from a portion of the mRNA transcriptome accumulate in a state that is sufficiently stable for them to be detected by these assays.

A role for cytoplasmic capping in maintaining the steady-state level of some mRNAs

The absence of transcripts from the induced set in RNA from K294A-expressing cells was unexpected, and suggested that the uncapped forms of these RNAs were degraded under conditions of reduced/inhibited cytoplasmic capping. This was supported by quantitative analysis of the microarray data, which showed a mean 0.57-fold decrease in their log expression in K294A-expressing cells compared to a mean 0.19-fold decrease for all other transcripts ($p = 2 \cdot 10^{-173}$). This analysis also identified another group of transcripts that declined more in K294A-expressing cells even though there was no evidence from the microarray data for uncapped forms of these (Table S2). The most straightforward interpretation of these data was that these were rapidly degraded when cytoplasmic capping was inhibited. The corollary to this is cytoplasmic capping plays a role in maintaining steady state levels of these mRNAs.

To test this we examined the impact of knocking down Xrn1 (Fig. 4A) on the relative amount of 3 of the transcripts that showed the greatest reduction in K294A-expressing cells, MSTN, TLR1 and S100Z. In each case, this increased the level of transcripts that were lost from K294A-expressing cells (Fig. 4B), indicating that uncapped forms of these transcripts were indeed rapidly degraded under conditions of inhibited cytoplasmic capping. Xrn1 knockdown had no impact on the expression of 2 control transcripts (BOP1, STRN4, Fig. 4C) and the increase in MAPK1 RNA indicates that its uncapped forms are also susceptible to 5'-3' decay. Our data are consistent with the non-canonical capping observed in Fejes-Toth et al., (2009), and are best explained by recapping of transcripts from which the cap has been lost by decapping or endonuclease cleavage, a process we have named cap homeostasis.

Cytoplasmic capping maintains the translation state of recapping targets

We next looked at the impact of inhibiting cytoplasmic capping on translation. The standard approach for studying the translation state of mRNAs is polysome profile analysis, and the absorbance profiles of uninduced and K294A-expressing cells showed translation was affected by inhibiting cytoplasmic capping (Fig. 5A). The 40S, 60S, 80S and polysome traces of control and K294A-expressing cells are superimposable, but inhibition of cytoplasmic capping resulted in a significant increase in 254 nm absorbing material in the non-translating mRNP fraction. Again qRT-PCR was used to analyze the distribution of recapping targets and controls, and in this and subsequent experiments results were normalized to a dephosphorylated luciferase RNA control that was added to each fraction. Inhibition of cytoplasmic capping shifted the recapping targets (EXOSC2, MAPK1,

POLR2B, STAT3, ZNF207) to the top of the gradient (Fig. 5B), a result consistent with changes in the absorbance profile. In contrast, there was no impact on the distribution of capped control mRNAs (BOP1 or LAMA5, Fig. 5C), thus indicating a role for cytoplasmic capping maintaining the translating state of mRNAs that are substrates for this process.

Non-translating mRNAs are uncapped

If the concept of cap homeostasis is correct, transcripts that accumulate in non-translating mRNPs should be uncapped. To test this we looked first at the overall impact of K294A expression on the distribution of 2 control and 2 recapping targets between the pooled mRNP and polysome fractions from the gradients in Fig. 5. Each of these samples included an internal control of dephosphorylated luciferase RNA and was analyzed by semi-quantitative RT-PCR using the same primers as in Fig. 5B and C. The products were separated by gel electrophoresis and the quantified results are shown beneath each lane (Fig. 6A). K294A expression had no impact on the distribution of control transcripts (LAMA5, BOP1); however, in the same cells approximately half of the recapping targets (ZNF207, MAPK1) moved from polysomes to the mRNP fraction. This experiment was repeated in Fig. 6B with the exception that mRNPs were recovered on discontinuous sucrose gradients (Otsuka and Schoenberg, 2008). Dephosphorylated (i.e. Xrn1-resistant) luciferase RNA was added to each preparation, and the recovered RNA was treated with Xrn1 to degrade uncapped RNAs. As in Fig. 6A ZNF207 and MAPK1 mRNAs accumulate in the mRNP fraction of K294A-expressing cells, and based on Xrn1 susceptibility virtually all of the relocated transcripts are uncapped. These data indicate a role for cytoplasmic capping in maintaining the translation state of these mRNAs and support the concept of cap homeostasis.

Properties of the re-capping target transcripts

To determine if their protein products link targets of cytoplasmic capping to particular pathways or cellular processes we performed gene ontology analysis using the DAVID Functional Annotation Clustering tool. Four cluster groupings stood out from this analysis (Fig. 7A and Table S3). Transcripts in the uninduced and common sets were significantly enriched for Nucleotide Binding and Protein Localization, and they also showed some enrichment for RNA Localization. Interestingly, the recapping targets in these sets included a number of RNA metabolic proteins that are linked to motor neuron diseases (FUS, GLE1) and Fragile X syndrome (FMR1), several of the CNOT proteins, HNRNPD (Auf1), and both exosome subunits (EXOSC2, 4, 9) and exosome-associated 3' exonucleases (EXOSC10, DIS3). The capping inhibited transcript set was further enriched for transcripts associated with Nucleotide Binding, Protein Localization and RNA Localization, and of the 3 transcript sets was the only ones enriched for proteins associated with the Mitotic Cell Cycle. The representation of recapping targets in these ontological groupings is consistent with previously published biological data in Otsuka et al. (2009) showing reduced ability of cells to recover from stress when cytoplasmic capping was blocked.

We next sought to determine if there were common sequence elements that might define any or all of the 3 transcript populations. Computational approaches identified microRNA binding sites in the 3'-UTRs of the genes corresponding to each of the transcript groups, and in general there were a greater number of these sites in cytoplasmic capping targets than the rest of the mRNA transcriptome. However, no single miRNA or group of miRNAs stood out as a defining feature. We then focused on the AU-rich elements (ARE) as another group of cis-acting sequences affecting mRNA metabolism. AREs stimulate decapping (Li and Kiledjian, 2010), and the turnover of ARE-containing mRNAs is controlled by the binding of destabilizing proteins (eg. tristetraprolin ZPF36; butyrate response factor 1 and 2, ZPF36L1 and 2), and stabilizing proteins such as HuR (reviewed in (Schoenberg and

Maquat, 2012). AREs also have an impact on translation efficiency, and tristetraprolin has been reported to inhibit translation of ARE-containing mRNA through interaction with p54/RCK (Qi et al., 2012).

There are 3 major classes of AREs; class I has a single 3'-UTR copy of the AUUUA pentamer, class II has multiple overlapping runs of AUUUA, and class III elements are generally U-rich but lack AUUUA. We limited our search to genes in the ARESite database (Gruber et al., 2011) having one or more AUUUA pentamers in their 3'-UTR, and by excluding class III AREs this analysis may underestimate the presence of AREs in target mRNAs. The results of this analysis are shown in Fig. 7B. Each of the transcript sets is enriched for AUUUA pentamers, with a median of 3 in the uninduced and capping inhibited sets and 4 in the common pool (upper panel). This compares to a median of 1 AUUUA pentamer in transcripts of the background genome. A comparison of these genes as a function of the number of AUUUA pentamers is shown in the lower panel of Fig. 7B. Sixty-five percent of the genes in the background genome have 1 AUUUA compared to 78–81% of the genes for each of the transcript sets. These differences become more apparent with increasing number of AUUUA pentamers, with 51–57% of target genes having 3 or more AUUUA repeats compared to 37% of the background genome. All of these are statistically significant ($p < 0.001$). These findings are consistent with the function of AREs in translation and mRNA decay, and suggest a role for sequences in the 3'-UTR in defining the scope of cytoplasmic capping targets.

Discussion

We reasoned that the best way to definitively identify cytoplasmic capping targets would be based on the accumulation of uncapped transcripts as a consequence of inhibiting this process, and in the current study this was done using a catalytically-inactive form of capping enzyme (K294A) that is restricted to the cytoplasm and whose overexpression interfered with the ability of cells to recover from stress (Otsuka et al., 2009). One of the modifications to this protein interferes with binding of the kinase that generates a diphosphate capping substrate from RNA with 5'-monophosphate ends. The ends of any uncapped mRNAs that accumulate under these conditions should have a 5'-monophosphate, making them susceptible to degradation by Xrn1. Exon arrays were then used to monitor changes across each transcript. The vast majority of the mRNAs showed no susceptibility to Xrn1 regardless of K294A expression, a result we interpret as indicative of them being fully capped. 2666 transcripts were found to have some inherent degree of Xrn1 susceptibility (the uninduced set), 675 transcripts were identified as having uncapped forms only in K294A-expressing cells (the capping inhibited set, and 835 transcripts with some degree of Xrn1 susceptibility were identified in both control and K294A-expressing cells (the common set). The heat maps in Fig. 1C–E provide graphic evidence for the accumulation of uncapped transcripts, and the impact of inhibiting cytoplasmic capping is most evident for the common set (Fig. 1D), which is the only case where the same transcripts could be compared between control and K294A-expressing cells.

Four different approaches were used to assess the impact of K294A expression on the cap status of targets identified in Fig. 1, three of which were based on the accumulation of 5'-monophosphate ends (Fig. 2 and Fig. 3A) and one of which was based on the presence or absence of a cap (Fig. 3B). The results of 5'-RACE in Fig. 3B raise some potentially important issues. RACE products for each of the recapping targets were more prominent when their corresponding RNA was recovered from K294A-expressing cells, but in the case of SARS and ZNF207 some of these were shorter than that anticipated for intact mRNAs, a result that is consistent with some degree of 5' end trimming. The final evidence that uncapped transcripts accumulate in cells expressing K294A came from their differential

exclusion from a cap affinity column. The particular approach used here consisted of glutathione Sepharose bound with a heterodimer of GST-eIF4E and the eIF4E-binding domain of eIF4G, a combination that increases cap binding efficiency (Imataka et al., 1998).

We anticipated that the uncapped transcripts found in uninduced cells would be a subset of a larger body of uncapped RNAs that would accumulate when cytoplasmic capping was inhibited. Instead all but those of the common set were missing from RNA of K294A-expressing cells, and the steady state levels of mRNAs from the uninduced set were lower in K294A-expressing cells than in control cells. This may explain the difference in regression lines in Supplemental Fig. S1A. These data also implied that interference with cytoplasmic capping makes some transcripts more susceptible to degradation, a result that was confirmed by their stabilization following Xrn1 knockdown (Fig. 4). This was not restricted to transcripts of the uninduced target set as steady-state level of MAPK1 was also increased by Xrn1 knockdown. A cyclical process of decapping and recapping that is inhibited by overexpression of K294A best explains these data and those in Fig. 5 and 6. We term this process cap homeostasis. Such cyclical changes are consistent with the large increase in 254 nm absorbing material at the top of the gradient in Fig. 5A and the redistribution of uncapped forms of recapping targets to non-translating mRNP. Moreover, the lack of global changes in the ribosome-bound mRNAs is consistent with results in Fig. 1 showing cytoplasmic capping impacts only a portion of the mRNA transcriptome.

The results presented here raise many questions. Some of the targets are linked to motor neuron diseases (eg. FUS, GLE1, Kolb et al., 2010), others are linked to cancer and inflammatory disorders (eg. VEGF). While the features that determine whether a particular mRNA is a substrate for cytoplasmic capping have yet to be determined the targets we identified are enriched for microRNA binding sites and AU-rich elements, both of which function in cap-dependent silencing (Zdanowicz et al., 2009; Qi et al., 2012). Both, microRNA silencing and ARE-mediated mRNA decay, are associated with poly(A) shortening, but this is not absolute (Bazzini et al., 2012; Djuranovic et al., 2012). Many of the transcripts we identified as targets of cytoplasmic capping (eg. zinc finger proteins) were also identified in Yang et al. (2011) in that portion of the mRNA transcriptome that was not recovered on oligo(dT). Since binding of poly(A) RNA to oligo(dT) is dependent on temperature and salt conditions (Murray and Schoenberg, 2008) it is possible their poly(A)-minus RNAs in fact have short poly(A) tails. We previously described a poly(A)-limiting element (PLE) that both restricts the length of poly(A) to <20 nucleotides (Das Gupta et al., 1998) and functionally substitutes for a long poly(A) tail in supporting translation (Peng and Schoenberg, 2005). Interestingly, one of the recapping targets is HIVP2, an mRNA we showed previously to have a PLE and a short poly(A) tail (Gu et al., 1999). Although more needs to be done to analyze the relationship between cytoplasmic capping and regulated polyadenylation this raises the possibility that other mRNAs have similar PLE-like elements, and recapping may be all that is required to restore their uncapped forms to the translating pool.

Cap homeostasis raises the possibility of a broad role for cytoplasmic capping in the mRNP cycle. Much has been written about the cycling of mRNAs between active (ie. translating) and inactive states and the function of visible and submicroscopic RNP complexes in this process. P bodies, neuronal granules, chromatoid bodies and maternal RNA granules all contain decapping enzymes, p54/RCK, and mRNAs which can be returned to the translating pool under the appropriate stimuli. Although the cap and cap-binding proteins are key factors in the silencing process nothing is known about the cap status of silenced or stored mRNAs. Our results provide the first evidence that non-translating mRNAs can accumulate in an uncapped state, and raise the possibility that decapping without degradation might be used to maintain some transcripts in 'deep hibernation', from which they may be

reawakened by cytoplasmic capping. Such a mechanism might be particularly useful for maintaining the non-translating state of maternal mRNAs and neuronal mRNAs as they move from the cell body to dendrites.

While the gene ontology analysis in Fig. 7A suggests that cytoplasmic capping plays a role in a number of cellular processes much remains to be done to determine the full scope of its role in gene expression. Transcripts with GO terms linked to the mitotic cell cycle are only seen in the capping inhibited set, and while it is premature to interpret functionality, these are also the transcripts that appear to be most stable in an uncapped state and to accumulate uncapped in non-translating mRNP. We showed previously that overexpression of K294A inhibits the ability of cells to recover from arsenite stress (Otsuka et al., 2009), and future work will determine if some of these are stored uncapped, for example in P bodies or stress granules, and require cytoplasmic capping to reactivate their translation. It will be equally important to determine where in the transcript the cap is added, and work is in progress to apply deep sequencing to the identification of these sites. We also have yet to determine if there are cis-acting elements or features other than the ones that were identified here that function in identifying substrates for cytoplasmic capping. Finally, Thoma et al. (2001) provided evidence for translation of proteins from sequences downstream of antisense-targeted cleavage sites. The mechanism responsible for this was not determined, but results presented here raise the possibility that these were recapped, and cytoplasmic capping may have a broader role in facilitating the synthesis of N-terminally truncated forms of some proteins.

Experimental Procedures

Cell culture

The establishment, growth and properties of tetracycline-inducible U2OS cells stably transfected with pcDNA4/TO/myc-K294 Δ NLS+NES-Flag (referred to here as K294A) are described in (Otsuka et al., 2009). These express a nonfunctional form of murine capping enzyme in which the active site lysine is changed to alanine. Its expression is restricted to the cytoplasm by deleting the 4 amino acid nuclear localization signal and addition of the HIV Rev nuclear export signal. In all of the experiments here, expression was induced by culturing cells for 24 hr in medium containing 1 μ g/ml of doxycycline except for polysome fractionation experiments, wherein cells were induced for 48 h. All the experiments were carried out in triplicate cultures.

Preparation of cytoplasmic RNA and poly(A) selection

Cells were washed twice in chilled phosphate-buffered saline (PBS), recovered by centrifugation at 100 xg and resuspended in 3 volumes of RSB buffer (10 mM Tris-HCl, pH 8.0, 10 mM NaCl, 2 mM EDTA, 0.5% NP-40, with the addition of 1 mM dithiothreitol and 800 units/ml of RNaseOUT (Invitrogen)). These were incubated on ice for 10 min with intermittent resuspension, then centrifuged at 1000 xg at 4°C for 10 min. Cytoplasmic RNA was recovered from the supernatant using Trizol (Invitrogen) as directed by the manufacturer. 5 μ g total cytoplasmic RNA was treated with 1 unit of DNase I (Invitrogen) and where necessary poly(A) RNA was selected using Dynabeads® mRNA DIRECT™ Kit (Invitrogen) as per the manufacturer's instructions. For RNA denaturation, samples were heated at 65°C for 5 min followed by snap chilling on ice.

Microarrays

10 μ g of cytoplasmic RNA from individual cultures was treated with 1 unit of DNase I and ribosomal RNA was removed by two rounds of RiboMinus™ (Invitrogen) selection. 0.6 μ g of selected RNA was heat denatured and either analyzed directly or treated for 2 hr at 37°C

with 5 units of Xrn1 (New England Biolabs) to partially degrade uncapped RNA. The reaction was terminated by heating at 70°C for 10 min, and fluorescently labeled cDNAs from biological triplicate samples were hybridized to individual Affymetrix Human Exon 1.0 ST microarrays. The exon array data was normalized with the standard RMA algorithm from the Oligo package for R from the Bioconductor suite and recorded as log₂ expression. Microarray data has been submitted to GEO (Accession number GSE36729).

Validation of uncapped transcripts

Uncapped transcripts identified by microarrays were validated by 5' RACE, susceptibility to degradation *in vitro* by Xrn1, ligation-mediated isolation (Jiao et al., 2008), and cap-based separation, details of which are presented in Supplemental Experimental Procedures. To determine the fold change due to K294A overexpression, transcript levels were normalized to those of uninduced samples. The data represent three independent culture replicates. Statistical comparison was performed by paired two-tailed Student's t-test (* p<0.05).

Xrn1 knockdown

Control and K294A cells were transfected with 20 nM Xrn1 siRNA (Origene) using Lipofectamine™ RNAiMAX Transfection Reagent (Invitrogen). Forty-eight hours later doxycycline (1 µg/ml) was added to one half of the cultures to induce K294A expression, and cells were harvested 24 hr later. The efficiency of Xrn1 knockdown was monitored by western blotting with rabbit anti-Xrn1 antibody (Santa Cruz). Cytoplasmic RNA was recovered and assayed for target gene expression by real time PCR using primers listed in Supplemental Experimental Procedures.

Polysome Fractionation, RNA quantitation & Xrn1 susceptibility of mRNPs

Cells were lysed in buffer containing 15 mM Tris-HCl pH 7.5, 10 mM MgCl₂, 150 mM KCl, 500 µg/ml cycloheximide, 0.5% Triton X-100, protease inhibitor cocktail (1:100 dilution from Sigma), phosphatase inhibitor cocktails 2 & 3 (1:100 dilution from Sigma), 2 mM sodium orthovanadate, 1 mM phenylmethylsulfonyl fluoride and 1 U/µl of RNasin (Promega). 300 µl of cytoplasmic extract was layered onto 10–50% linear gradients prepared in buffer containing, 15 mM Tris-HCl (pH 7.5), 10 mM MgCl₂, 150 mM KCl, and 100 µg/ml cycloheximide. These were centrifuged at 210,000 xg in a Sorvall TH641 rotor for 3 hr at 4°C. 0.5 ml fractions were collected from the top with continuous monitoring of the absorbance at 254 nm. 0.5 ng of an Xrn1-resistant form of polyadenylated (A₉₈) firefly luciferase RNA was added as a normalization control to 200 µl of each fraction. The luciferase transcript was made resistant to Xrn1 by removing 5' phosphates with shrimp alkaline phosphatase. RNA recovered with Trizol reagent was stored in DEPC-treated water. cDNA was prepared from each fraction using the Superscript III cDNA Synthesis kit (Invitrogen) with random hexamer priming, and transcripts were quantified by SYBR green based qRT-PCR using primers located near the 3' end of each of the transcripts (see the primer table in Supplemental Experimental Procedures). Alternatively, to demonstrate the accumulation of target transcripts in mRNPs, the linear gradient fractions 1, 3, & 5 were pooled as mRNPs and fractions 13, 15, 17, 19 & 21 were pooled to form polysomal fractions. These pools were used for cDNA synthesis and semiquantitative PCR using 3' end primers. The products were analyzed on 2% agarose gel in 1X TBE using Quantity One 1-D gel imaging software (Biorad). The cap status of transcripts in the mRNP fraction was determined by treating RNA from the mRNP pool with Xrn1, followed by semiquantitative RT-PCR using primers located near the 5' ends of the target transcripts. The products of these reactions were analyzed on 2% agarose gel in 1X TBE.

Supplementary Material

Refer to Web version on PubMed Central for supplementary material.

Acknowledgments

We thank Nahum Sonenberg and Jerry Pelletier (McGill University, Canada) for plasmids, Juan Gutierrez (Ohio State Mathematical Biosciences Institute) for his help with bioinformatics, and Daniel L. Kiss and other members of the Schoenberg lab for their helpful comments and discussion. We also acknowledge the support for the Microarray Shared Resource of the Ohio State Comprehensive Cancer Center. Research reported in this publication was supported by the National Institute of General Medical Sciences of the National Institutes of Health under award numbers R01GM084177 and R01GM038277. The content is solely the responsibility of the authors and does not necessarily represent the official views of the National Institutes of Health.

References

- Anderson P, Kedersha N. Stressful initiations. *J Cell Sci.* 2002; 115:3227–3234. [PubMed: 12140254]
- Bazzini AA, Lee MT, Giraldez AJ. Ribosome profiling shows that miR-430 reduces translation before causing mRNA decay in Zebrafish. *Science.* 2012; 336:233–237. [PubMed: 22422859]
- Bremer KA, Stevens A, Schoenberg DR. An endonuclease activity similar to *Xenopus* PMR1 catalyzes the degradation of normal and nonsense-containing human beta-globin mRNA in erythroid cells. *RNA.* 2003; 9:1157–1167. [PubMed: 12923263]
- Chu C, Shatkin AJ. Apoptosis and autophagy induction in mammalian cells by siRNA knockdown of mRNA capping enzymes. *Mol Cell Biol.* 2008; 28:5829–36. [PubMed: 18678651]
- Das Gupta J, Gu H, Chernokalskaya E, Gao X, Schoenberg DR. Identification of two cis-acting elements that independently regulate the length of poly(A) on *Xenopus* albumin pre-mRNA. *RNA.* 1998; 4:766–776. [PubMed: 9671050]
- Djuranovic S, Nahvi A, Green R. miRNA-mediated gene silencing by translational repression followed by mRNA deadenylation and decay. *Science.* 2012; 336:237–240. [PubMed: 22499947]
- Fejes-Toth K, Sotirova V, Sachidanandam R, Assaf G, Hannon GJ, Kapranov P, Foissac S, Willingham AT, Duttagupta R, Dumais E, Gingeras TR. Post-transcriptional processing generates a diversity of 5'-modified long and short RNAs. *Nature.* 2009; 457:1028–1032. [PubMed: 19169241]
- Gregory BD, O'Malley RC, Lister R, Urich MA, Tonti-Filippini J, Chen H, Millar AH, Ecker JR. A link between RNA metabolism and silencing affecting Arabidopsis development. *Dev Cell.* 2008; 14:854–866. [PubMed: 18486559]
- Gruber AR, Fallmann J, Kratochvill F, Kovarik P, Hofacker IL. AREsite: a database for the comprehensive investigation of AU-rich elements. *Nucleic Acids Res.* 2011; 39:D66–9. [PubMed: 21071424]
- Gu H, Das GJ, Schoenberg DR. The poly(A)-limiting element is a conserved cis-acting sequence that regulates the length of poly(A) on nuclear pre-mRNAs. *Proc Natl Acad Sci USA.* 1999; 96:8943–8948. [PubMed: 10430875]
- Gu M, Lima CD. Processing the message: structural insights into capping and decapping mRNA. *Curr Opin Struct Biol.* 2005; 15:99–106. [PubMed: 15718140]
- Hu W, Sweet TJ, Chamnongpol S, Baker KE, Collier J. Co-translational mRNA decay in *Saccharomyces cerevisiae*. *Nature.* 2009; 461:225–229. [PubMed: 19701183]
- Imataka H, Gradi A, Sonenberg N. A newly identified N-terminal amino acid sequence of human eIF4G binds poly(A)-binding protein and functions in poly(A)-dependent translation. *EMBO J.* 1998; 17:7480–7489. [PubMed: 9857202]
- Jiao X, Xiang S, Oh C, Martin CE, Tong L, Kiledjian M. Identification of a quality-control mechanism for mRNA 5'-end capping. *Nature.* 2010; 467:608–611. [PubMed: 20802481]
- Jiao Y, Riechmann JL, Meyerowitz EM. Transcriptome-wide analysis of uncapped mRNAs in Arabidopsis reveals regulation of mRNA degradation. *Plant Cell.* 2008; 20:2571–2585. [PubMed: 18952771]

- Karginov FV, Cheloufi S, Chong MMW, Start A, Smith AD, Hannon GJ. Diverse endonucleolytic cleavage sites in the mammalian transcriptome depend on microRNAs, Drosha and additional nucleases. *Mol Cell*. 2010; 38:781–788. [PubMed: 20620951]
- Kolb SJ, Sutton S, Schoenberg DR. RNA processing defects associated with diseases of the motor neuron. *Muscle Nerve*. 2010; 41:5–17. [PubMed: 19697368]
- Li Y, Kiledjian M. Regulation of mRNA decapping. *Wiley Interdiscip Rev RNA*. 2010; 1:253–265. [PubMed: 21935889]
- Lim SK, Maquat LE. Human beta-globin mRNAs that harbor a nonsense codon are degraded in murine erythroid tissues to intermediates lacking regions of exon I or exons I and II that have a cap-like structure at the 5' termini. *EMBO J*. 1992; 11:3271–3278. [PubMed: 1324170]
- Lim SK, Sigmund CD, Gross KW, Maquat LE. Nonsense codons in human beta-globin mRNA result in the production of mRNA degradation products. *Mol Cell Biol*. 1992; 12:1149–1161. [PubMed: 1545796]
- Mercer TR, Dinger ME, Bracken CP, Kolle G, Szubert JM, Korbie DJ, Askarian-Amiri ME, Gardiner BB, Goodall GJ, Grimmond SM, Mattick JS. Regulated post-transcriptional RNA cleavage diversifies the eukaryotic transcriptome. *Genome Res*. 2010; 20:1639–1650. [PubMed: 21045082]
- Mullen TE, Marzluff WF. Degradation of histone mRNA requires oligouridylation followed by decapping and simultaneous degradation of the mRNA both 5' to 3' and 3' to 5'. *Genes Dev*. 2008; 22:50–65. [PubMed: 18172165]
- Murray EL, Schoenberg DR. A+U-rich instability elements differentially activate 5'-3' and 3'-5' mRNA decay. *Mol Cell Biol*. 2007; 27:2791–2799. [PubMed: 17296726]
- Murray EL, Schoenberg DR. Assays for determining poly(A) tail length and the polarity of mRNA decay in mammalian cells. *Methods Enzymol*. 2008; 448:483–504. [PubMed: 19111191]
- Ni T, Corcoran DL, Rach EA, Song S, Spana EP, Gao Y, Ohler U, Zhu J. A paired-end sequencing strategy to map the complex landscape of transcription initiation. *Nat Methods*. 2010; 7:521–527. [PubMed: 20495556]
- Otsuka Y, Kedersha NL, Schoenberg DR. Identification of a cytoplasmic complex that adds a cap onto 5'-monophosphate RNA. *Mol Cell Biol*. 2009; 29:2155–2167. [PubMed: 19223470]
- Otsuka Y, Schoenberg DR. Approaches for studying PMR1 endonuclease-mediated mRNA decay. *Methods Enzymol*. 2008; 448:241–263. [PubMed: 19111180]
- Peng J, Schoenberg DR. mRNA with a <20 nt poly(A) tail imparted by the poly(A)-limiting element is translated as efficiently in vivo as long poly(A) mRNA. *RNA*. 2005; 11:1131–1140. [PubMed: 15929942]
- Qi MY, Wang ZZ, Zhang Z, Shao Q, Zeng A, Li XQ, Li WQ, Wang C, Tian FJ, Li Q, Zou J, Qin YW, Brewer G, Huang S, Jing Q. AU-Rich element-dependent translation repression requires the cooperation of tristetraprolin and RCK/P54. *Mol Cell Biol*. 2012; 32:913–928. [PubMed: 22203041]
- Schoenberg DR. Mechanisms of endonuclease-mediated mRNA decay. *Wiley Interdisc Rev: RNA*. 2011; 2:582–600.
- Schoenberg DR, Maquat LE. Re-capping the message. *Trends Biochem Sci*. 2009; 34:435–442. [PubMed: 19729311]
- Schoenberg DR, Maquat LE. Regulation of cytoplasmic mRNA decay. *Nat Rev Genet*. 2012; 13:246–259. [PubMed: 22392217]
- Stevens A, Wang Y, Bremer K, Zhang J, Hoepfner R, Antoniou M, Schoenberg DR, Maquat LE. Beta-globin mRNA decay in erythroid cells: UG site-preferred endonucleolytic cleavage that is augmented by a premature termination codon. *Proc Natl Acad Sci USA*. 2002; 99:12741–12746. [PubMed: 12242335]
- Thoma C, Hasselblatt P, Kock J, Chang SF, Hockenjos B, Will H, Hentze MW, Blum HE, von WF, Offensperger WB. Generation of stable mRNA fragments and translation of N-truncated proteins induced by antisense oligodeoxynucleotides. *Mol Cell*. 2001; 8:865–872. [PubMed: 11684021]
- Yang L, Duff MO, Graveley BR, Carmichael GG, Chen LL. Genomewide characterization of non-polyadenylated RNAs. *Genome Biol*. 2011; 12:R16. [PubMed: 21324177]

Zdanowicz A, Thermann R, Kowalska J, Jemielity J, Duncan K, Preiss T, Darzynkiewicz E, Hentze MW. Drosophila miR2 primarily targets the m7GpppN cap structure for translational repression. *Mol Cell*. 2009; 35:881–888. [PubMed: 19782035]

Highlights

- mRNAs were identified that undergo cyclical loss and restoration of the cap
- Some recapping targets are destabilized when cytoplasmic capping is inhibited
- Cytoplasmic capping functions in cycling mRNA between polysomes and mRNPs
- In cells inhibited for cytoplasmic capping non-translating mRNA is stored uncapped

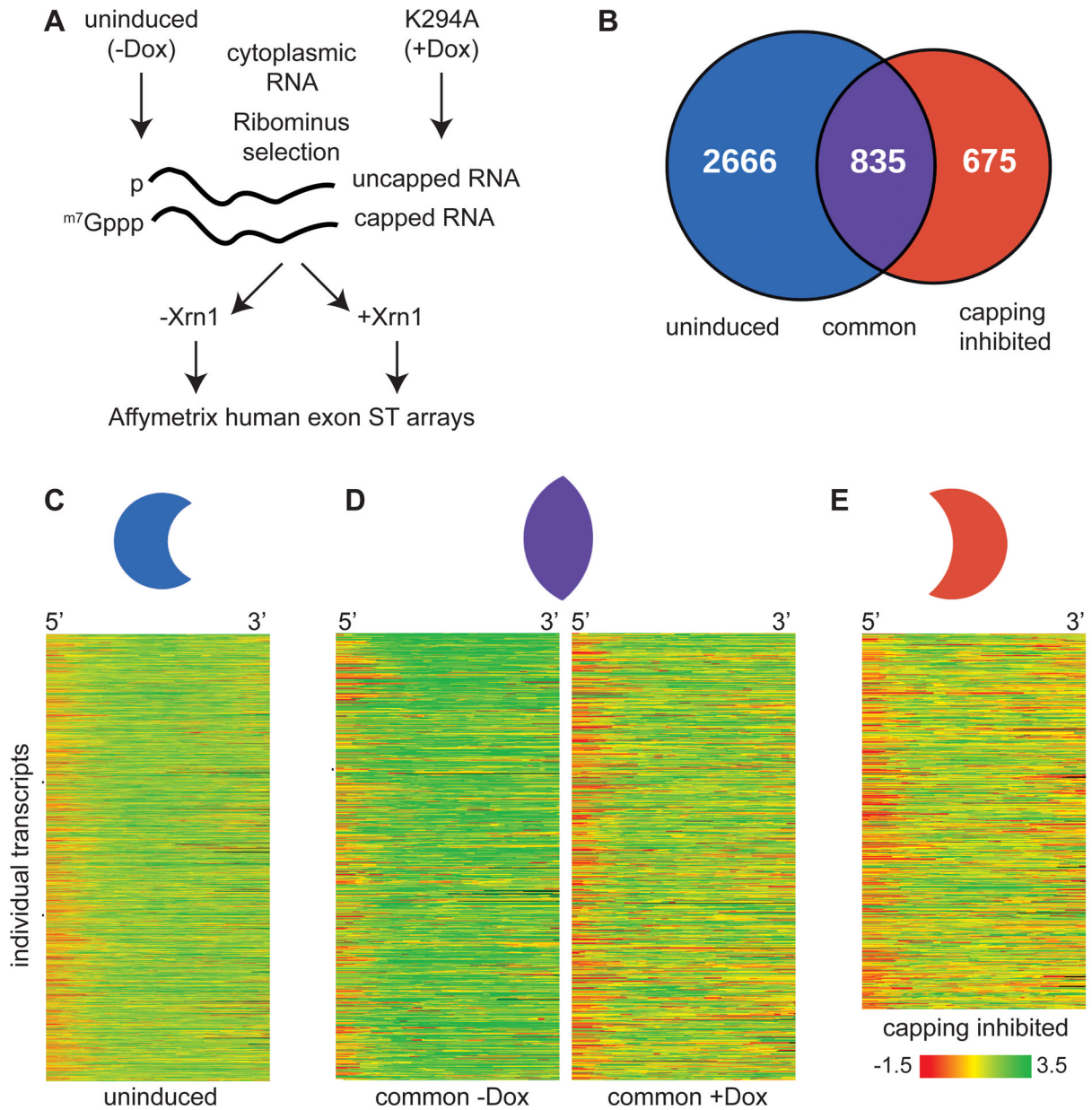


Figure 1. Identification of cytoplasmic capping targets

(A) The flowchart depicts the strategy used to identify uncapped transcripts from cells that were stably transfected with an inducible form of cytoplasmic capping enzyme in which the active site lysine was changed to alanine (K294A). Cytoplasmic RNA was isolated from triplicate cultures that were treated without and with doxycycline to induce K294A expression. After removal of ribosomal RNA one-half of each preparation was treated with Xrn1 to degrade uncapped RNA, and each preparation was analyzed on individual Affymetrix Human Exon ST 1.0 microarrays. (B) Venn diagram illustrating the number of transcripts identified as having uncapped forms only in cells in which K294A was not expressed (uninduced, blue), those having uncapped forms only in K294A-expressing cells (capping inhibited, red) and those that were identified in both populations (common, purple). The individual transcripts in each of these groups are listed in Table S1. (C,D,E) Heat maps of each of the transcript sets for uninduced, common and K294A datasets. Each line

represents the average difference in probe intensity as a function of Xrn1 digestion across the first 1500 nucleotides of individual transcripts. Different transcripts are represented in (C) and (E), however in (D) the same transcripts of the Common set are compared between control and K294A-expressing cells.

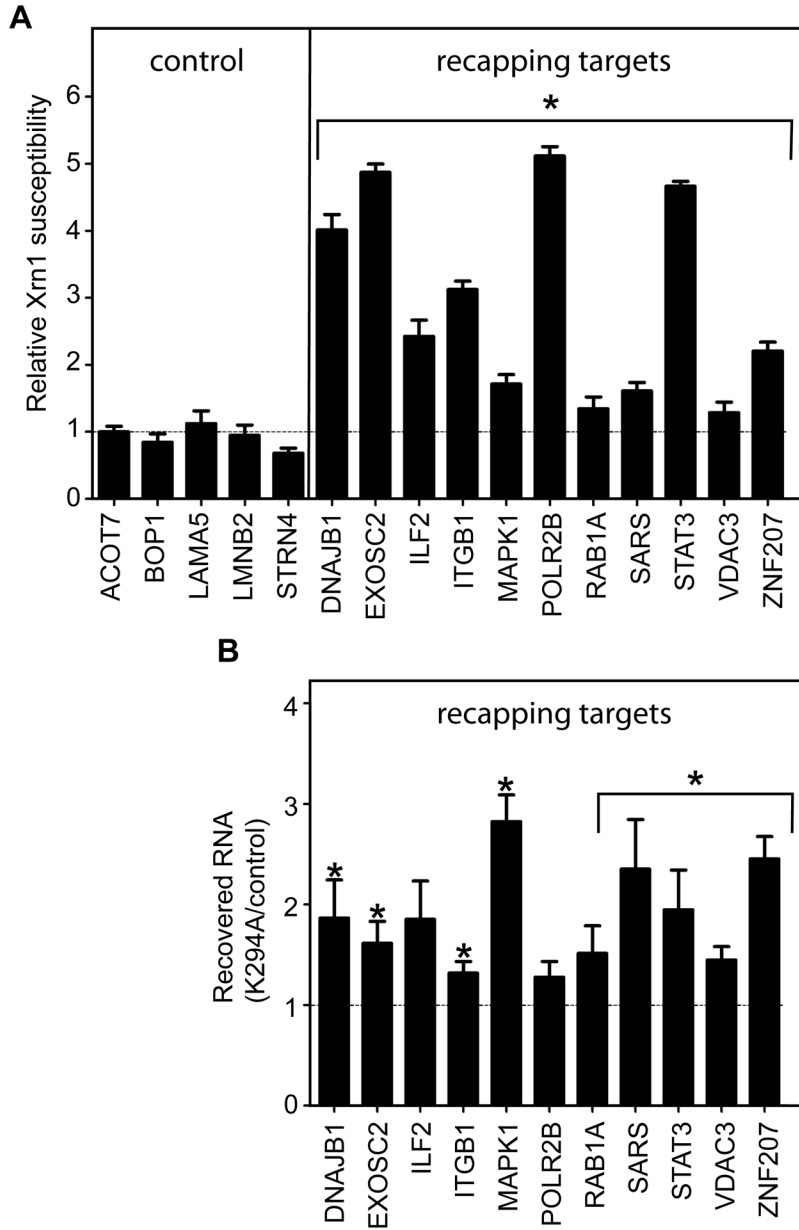


Figure 2. Validation of cytoplasmic capping enzyme targets based on changes in 5'-monophosphate ends

(A) Five controls and 11 transcripts that were identified as recapping targets in Fig. 1 were selected for validation of changes in cap status as a function of K294A expression. Poly(A)-selected RNA from triplicate cultures of control and K294A-expressing cells was treated \pm Xrn1 and analyzed by qRT-PCR using primers close to the 5' end of the transcripts (see Supplemental Materials and Methods). β -actin was used as an internal control and the change in Xrn1 susceptibility is presented as $\Delta X_{K294A}/\Delta X_{Control}$ ratio, where $\Delta X_{Control}$ is the relative loss of transcript 5' ends in control, and ΔX_{K294A} is their relative loss in K294A-expressing cells. A ratio of 1 indicates no change in Xrn1 susceptibility as a consequence of K294A expression and all of the results are normalized to this value. (B) Selective ligation-mediated recovery of uncapped transcripts as a function of K294A expression. Poly(A) selected cytoplasmic RNA from triplicate cultures of control and

K294A-expressing cells was ligated to an RNA adaptor. This was hybridized to a complementary biotinylated antisense DNA oligonucleotide, the duplex was recovered on streptavidin paramagnetic beads, and the recovered RNA was analyzed by qRT-PCR using the same primers as in (A). The C_t values for each gene were normalized against the internal control uncapped β -globin RNA present in each sample prior to ligation, and the normalized C_t value for RNA from control cells was arbitrarily set to 1. For (A) and (B) statistical significance (paired two-tailed Student's t-test (* $p < 0.05$)) was determined by comparing the values to those of control, which included relative standard deviations calculated from technical and biological replicates. The results represent the mean \pm standard deviation for 3 independent biological replicates.

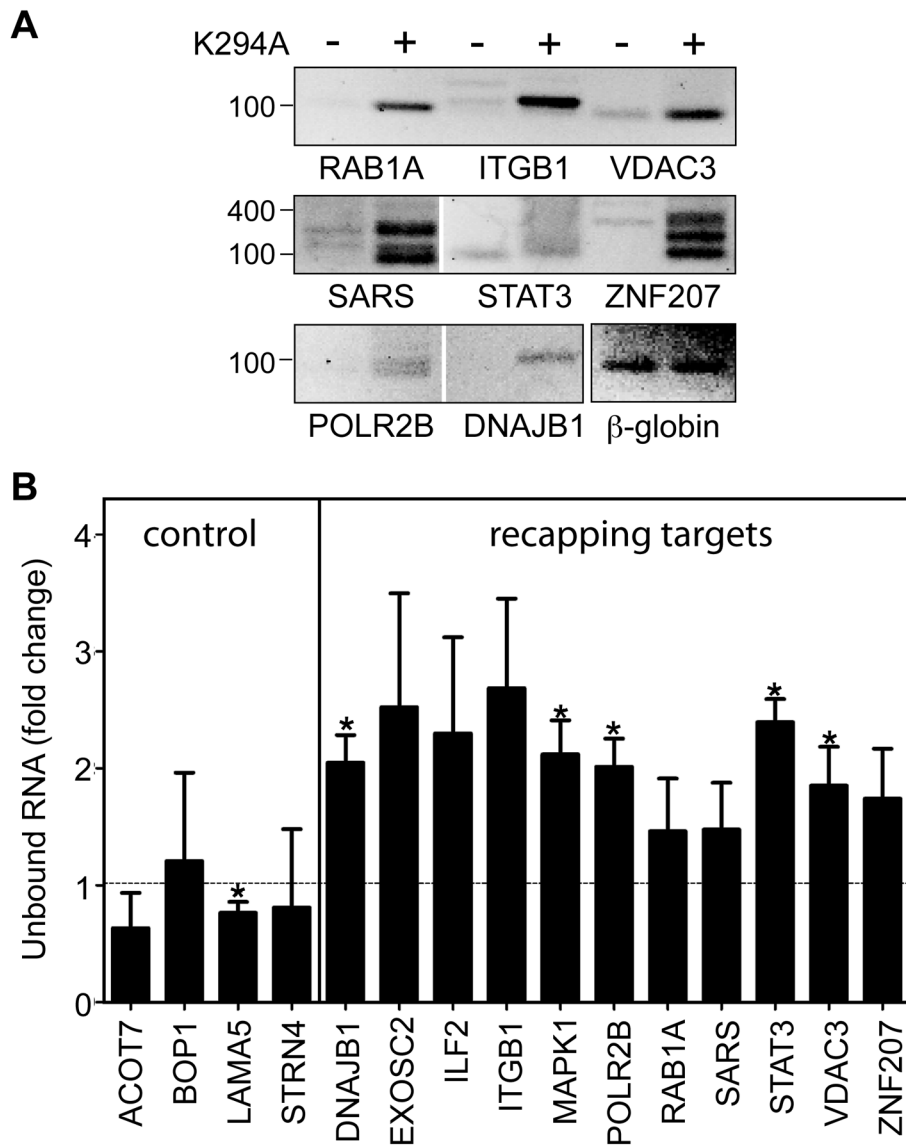


Figure 3. 5'-RACE and cap affinity chromatography confirm uncapped transcripts accumulate in K294A-expressing cells

(A) 5'-RACE was performed on the pooled primer-ligated RNAs from Figure 2B using a primer complementary to the ligated RNA adapter and a downstream primer within the body of each transcript. RACE products were separated on a 1.2% agarose gel and visualized by staining. The panel at the bottom right of the figure shows the 5'-RACE products of the internal uncapped β -globin mRNA control. (B) Cytoplasmic RNA from control and K294A-expressing cells was incubated with glutathione Sepharose bound with a heterodimer of GST-eIF4E plus GST-tagged eIF4E-binding domain of eIF4G. qRT-PCR was performed on unbound RNA using the same primers as in Figure 2, and C_t values for each transcript were normalized to the internal uncapped β -globin RNA control. The normalized C_t value for control samples was set to 1, and statistical analysis was performed as in Figure 2 (* $p < 0.05$). The results are presented as mean \pm standard deviation for 3 independent biological replicates.

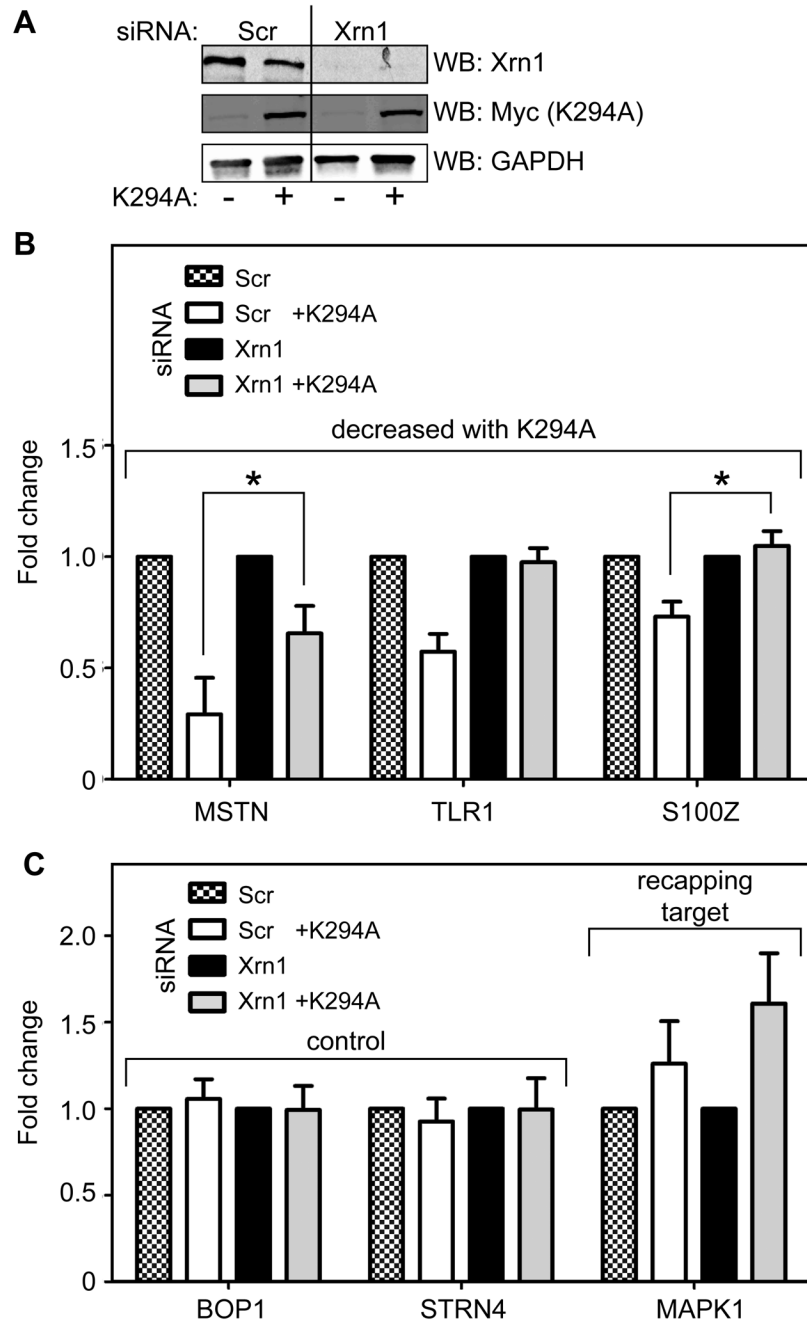


Figure 4. A role for cytoplasmic capping in maintaining transcript stability

(A) Cells were transfected with siRNAs against Xrn1 (Xrn1) or a scrambled control (Scr) prior to inducing K294A in half of the cultures. Western blotting with antibodies to Xrn1 and the Myc tag on K294A was used to assess the effectiveness of Xrn1 knockdown and K294A induction, and GAPDH was also analyzed as a loading control. (B) qRT-PCR was used to assess changes in the steady-state levels of 3 of the transcripts that showed the greatest degree of loss between control and K294A-expressing cells (see Supplemental Table S2), and the impact of Xrn1 knockdown on this. The relative amount of each transcript (MSTN and S100Z, * $p < 0.05$, paired two-tailed Student's t-test) was increased by knockdown of Xrn1 in K294A-expressing cells. (C) A similar analysis was performed on

two control transcripts (BOP1, STRN4), and one of the recapping targets analyzed in Figures 2 and 3 (MAPK1). In each of these analyses the level of a particular transcript in uninduced cells transfected with the scrambled control siRNA was arbitrarily set to one. Results in (B) and (C) are shown as the mean \pm standard deviation for 3 independent biological replicates.

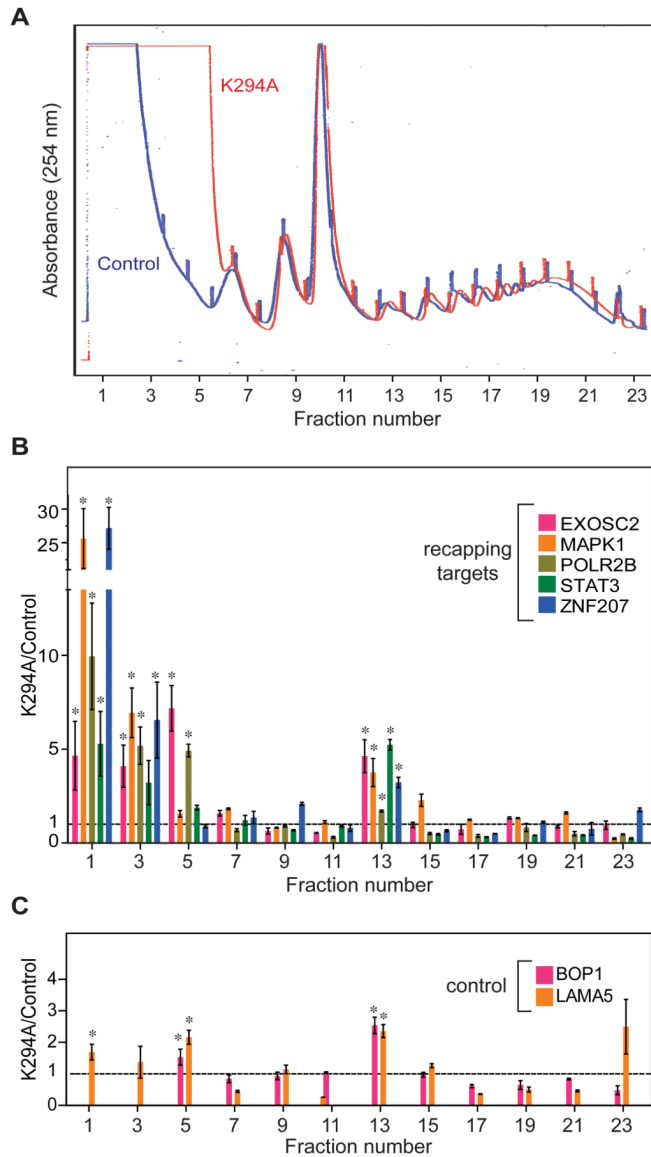


Figure 5. Expression of K294A alters the distribution of recapping targets between polysomes and non-translating mRNP

(A) Cytoplasmic extracts from control (blue) and K294A-expressing cells (red) were fractionated on 10–50% sucrose gradients. The gradients were collected from the top with continuous monitoring of absorbance at 254 nm. These profiles are representative of gradients done with extracts from 3 independent cultures. (B) Prior to isolating RNA each fraction received an equal amount of a dephosphorylated firefly luciferase RNA with a 98 nt poly(A) tail as a normalization control. RNA recovered from odd-numbered fractions of each gradient was analyzed as in Figures 2–4 by qRT-PCR using primers for 5 recapping targets (EXOSC2, MAPK1, POLR2B, STAT3, ZNF207). The primer sets in this experiment were located near the 3' end of each transcript (Supplemental Experimental Procedures) to avoid loss of signal from 5' end trimming, and results are presented as the amount of each transcript in a particular fraction from K294A-expressing cells compared to the transcript in the same gradient fraction from control cells. (C) The same analysis was performed as in (B) using primers for 2 control transcripts (BOP1, LAMA5). The results from individual

fractions were analyzed by paired two-tailed Student's t-test (* $p < 0.05$), and the data are presented as the mean \pm standard deviation from 3 independent replicates.

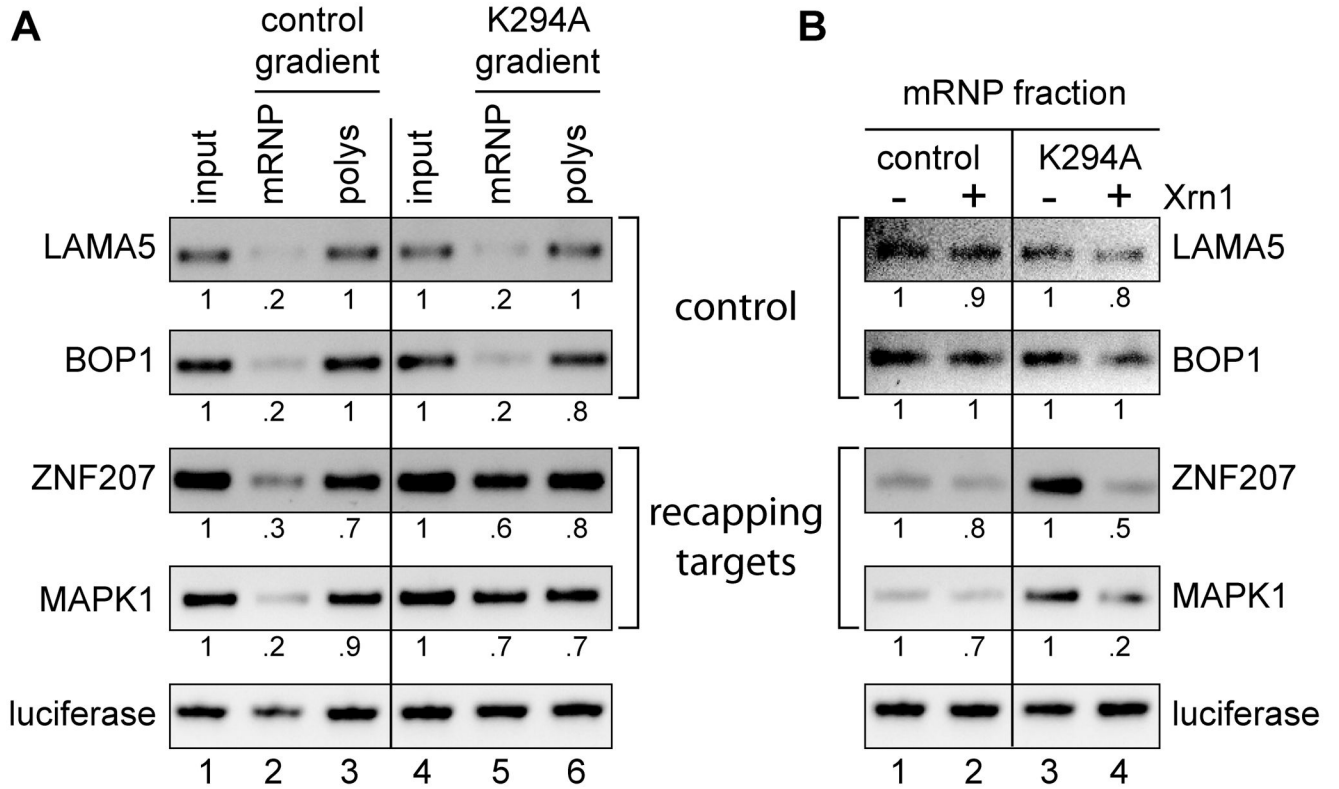
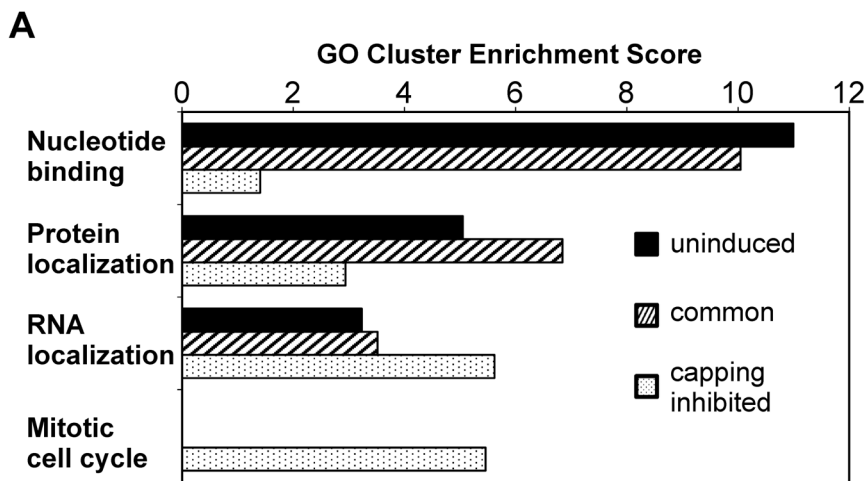


Figure 6. The recapping targets that accumulate in non-translating mRNP are uncapped

(A) RNA was recovered from each of the input cytoplasmic extracts from Figure 5 (input), and pooled mRNP (1,3,5) and polysome fractions (13,15,17,19,21) from each gradient. Each pool received an equal amount of dephosphorylated firefly luciferase RNA as an internal control prior to RNA purification, which was followed by cDNA synthesis, and the cDNAs were analyzed by semi-quantitative RT-PCR using the same 3'-weighted primers as in Figure 5(B and C). The products were separated on a 1.2% agarose gel and quantified using a BioRad GelDoc Imager and Quantity One 1-D gel analysis software. Results were normalized to the internal luciferase control. (B) Sucrose step gradients were used to recover mRNP fractions from triplicate cultures of control and K294A-expressing cells. An equal amount of dephosphorylated firefly luciferase RNA was added to each sample as an Xrn1-resistant control and the recovered RNA was treated Xrn1 to degrade uncapped transcripts. Individual samples were amplified by semi-quantitative RT-PCR using primers located near the 5' ends of two recapping targets (ZNF207, MAPK1) and two controls (BOP1, LAMA5), the pooled products were separated on a 1.2% agarose gel and visualized and quantified as in (A).



B

	Total #genes	Total #AUUUA	mean #AUUUA	median #AUUUA
whole genome	18562	59033	3.2	1
uninduced	1496	6984	4.7	3
common	493	2788	5.7	4
capping inhibited	368	1786	4.9	3
	minimum with 1-4 AUUUA (percent)			
	≥1	≥2	≥3	≥4
whole genome	12088 (65%)	8978 (48%)	6942 (37%)	5503 (30%)
uninduced	1169 (78%)	943 (63%)	765 (51%)	652 (44%)
common	405 (82%)	328 (66%)	280 (57%)	248 (50%)
capping inhibited	298 (81%)	240 (65%)	204 (55%)	172 (47%)

Figure 7. Properties of recapping targets

(A) Gene ontology analysis of transcripts in the uninduced, common and capping inhibited transcripts sets was performed using the NIH DAVID tool with default settings and high stringency. The top 4 cluster groupings are shown as a function of each of the transcript sets, with additional groupings in Supplemental Table S3. (B) A python script was developed to search the AREsite database for AUUUA elements present in the 3'-UTRs of the genes that correspond to the 55,662 Ensembl transcripts that were analyzed in Figure 1. The upper panel details the total number of AUUUA elements and the mean and median number of elements per transcript in each dataset, and in the lower panel these are broken down by the percentage of transcripts with different numbers of AUUUA elements.